CRYSTAL GROWTH & DESIGN
Article
pubs.acs.org/crystal

Organic Crystal Engineering with 1,4-Piperazine-2,5-diones. 8. Synthesis, Crystal Packing, and Thermochemistry of Piperazinediones Derived from 2-Amino-4,7-dialkoxyindan-2-carboxylic Acids

Kirk E. Wells, Robin A. Weatherhead, Francis N. Murigi, Gary S. Nichol, Michael D. Carducci, Hugh D. Selby, and Eugene A. Mash*

Department of Chemistry and Biochemistry, University of Arizona, Tucson, Arizona 85721, United States

Supporting Information

ABSTRACT: 1,4-Piperazine-2,5-diones possessing C_{2h} molecular symmetry and bearing four methoxy, ethoxy, butoxy, hexyloxy, octyloxy, nonyloxy, dodecyloxy, or octadecyloxy groups were synthesized from 2-amino-4,7-dialkoxyindan-2-carboxylic acids. Where possible, the piperazinediones were crystallized from appropriate solvents and the supramolecular organizations were determined by X-ray crystallography. In each case so studied, crystal assembly via three mutually orthogonal interactions, namely, $R_2^2(8)$ hydrogen bonding, arene perpendicular edge-to-center interactions, and alkyl chain interdigitation, was observed. The thermochemical properties of these compounds were studied by modulated differential scanning calorimetry. In most cases, one or more reversible thermal events were observed between room temperature and melting to an isotropic liquid. In the cooling cycle, freezing point temperatures were observed to decrease with increasing hydrocarbon chain length. This may be due to greater entropic penalties for hydrogen-bond association of molecules with longer hydrocarbon chains.

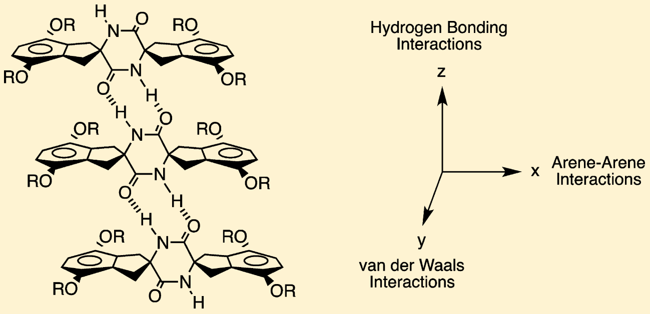

INTRODUCTION

The field of crystal engineering[1−6] seeks an understanding of weak intermolecular associative forces and strives for rational development of materials useful for a wide range of applications, for example, liquid crystal materials[7−9] for use in optical displays. We consider the molecular framework of pentacyclic molecules **1** suitable for use in an exploration of structural effects on weak intermolecular associative forces and an appropriate scaffold for the design of compounds that could possess useful bulk properties.[10−17] The conformational freedom of such molecules is restricted,[18] limiting the number of possible packing options. At the same time, attachment of functional groups to the scaffold can provide structural variability. For example, incorporation of alkoxy groups as in **2** endows the molecule with three chemically and spatially independent recognition elements (see Figure 1).

The central 1,4-piperazine-2,5-dione ring of **2** is known to favor formation of supramolecular "one-dimensional" tapes through reciprocal amide-to-amide $R_2^2(8)$ hydrogen bonding (*z*-axis, Figure 1).[19] Control of order in the second and third dimensions for hydrogen-bonded one-dimensional (1D) tapes of **2** depends on harnessing arene−arene interactions (*x*-axis) and van der Waals interactions (*y*-axis). van der Waals attractive interactions almost always contribute significantly to stabilization of the crystal structure as evidenced by the tendency of organic compounds to achieve closest packing in the solid state.[20−24] Various arene interaction types have been recognized as important, from the packing of small molecules to the stabilization of protein tertiary structures.[25,26] Parallel center-to-center association[27] is favored for arene rings that possess very different electron densities, as in cocrystals of arenes and perfluoroarenes.[28−31] Parallel edge-to-center association[27] also is responsive to changes in π electron density due to substituent effects.[31,32] Perpendicular edge-to-center associations[27] are often observed for unsubstituted arenes, as in the crystal structures of benzene,[33] naphthalene,[34] and anthracene,[35] among others. Both the nature and magnitude of perpendicular edge-to-center interactions have been questioned, but there is agreement that such interactions are stabilizing.[36−43]

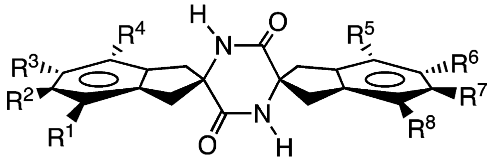

1

We previously observed that the crystal packing of compound **3a** (Figure 2, top) followed the assembly paradigm given in Figure 1.[44] Piperazinediones with topology similar to **3a** packed similarly.[45] Given these observations and the fact that alkyl chains longer than butyl generally adopt an extended zig−zag

Received: July 18, 2012
Revised: August 23, 2012
Published: August 24, 2012

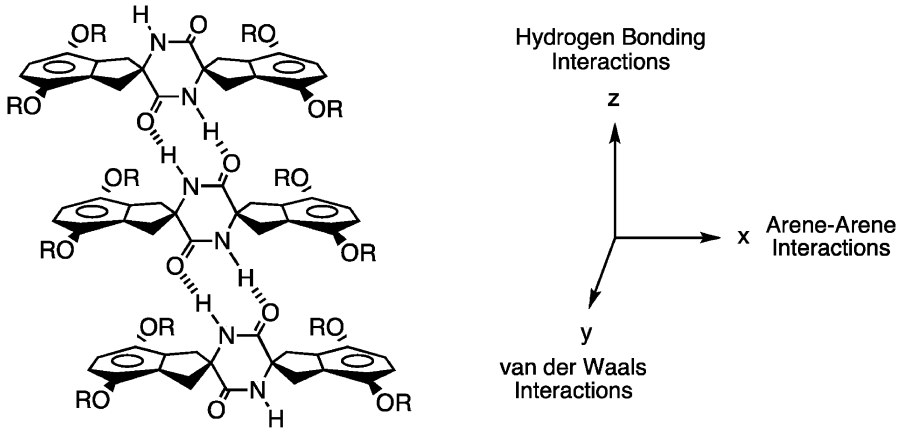

2

Figure 1. Directionality of propagation of chemically and spatially independent intermolecular recognition elements on piperazinedione scaffold **2**.

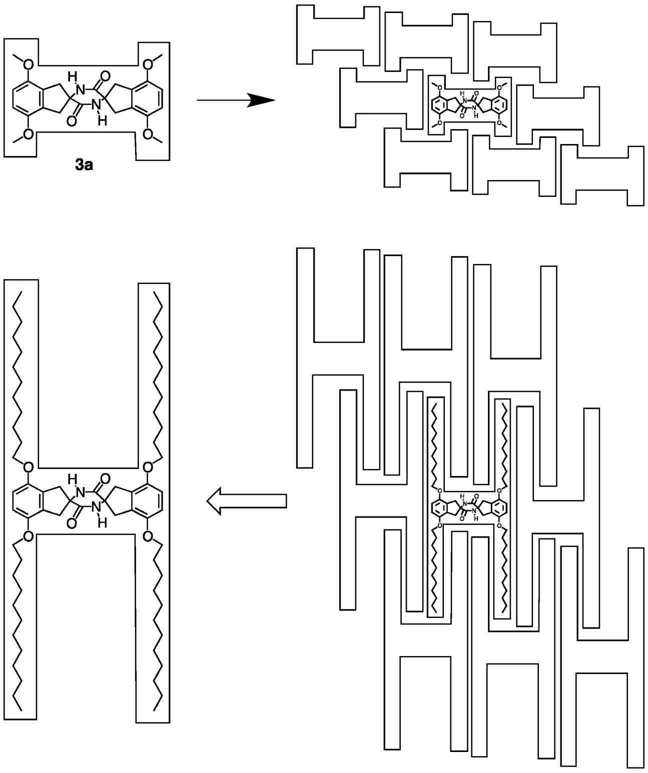

Figure 2. Top: Cartoon representations of the observed hydrogen-bonded tape cross-section (left) and crystal packing (right) viewed down the long axis of the tape for compound **3a**. Bottom: Cartoon representations of a hypothetical hydrogen-bonded tape cross-section (left) and crystal packing (right) viewed parallel to the long axis of the tape for **3g**, the dodecyloxy homologue of **3a**.

conformation and pack in either a parallel or an antiparallel fashion in the crystalline state,[46,47] we postulated that tapes formed from compounds related to **3a**, but with elongated cross sections due to extension of the alkyl chains (e.g., **3b**–**3h**), would pack via reciprocal amide hydrogen bonding, arene perpendicular edge-to-center interactions, and van der Waals-driven interdigitation of the alkyl chains in extended conformations (Figure 2, bottom).[48]

Molecules **3** possessing alkyl chains of sufficient length might exhibit liquid crystal properties. As a step toward examining this possibility, we report here on the synthesis and thermochemical properties of the set of tetraalkoxy-substituted piperazinediones **3b**–**3h**, and on the crystal structures of **3b**, **3c**, and **3g**.

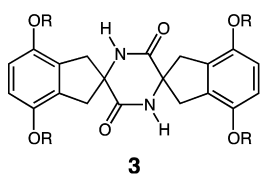

3

a R = CH_3
b R = CH_2CH_3
c R = $(CH_2)_3CH_3$
d R = $(CH_2)_5CH_3$
e R = $(CH_2)_7CH_3$
f R = $(CH_2)_8CH_3$
g R = $(CH_2)_{11}CH_3$
h R = $(CH_2)_{17}CH_3$

EXPERIMENTAL SECTION[49]

Syntheses of **3b** and **3d** provide representative examples of the synthetic methods employed. Details of the syntheses and characterizations of **3c** and **3e**–**h** appear in the Supporting Information that accompanies this article.

1,4-Diethoxy-2,3-dimethylbenzene (5b). Sodium metal (4.69 g, 204 mmol) was cut into slivers and washed with hexanes prior to suspension piecewise in absolute ethanol (150 mL). After complete reaction, 2,3-dimethylhydroquinone (**4**, 11.5 g, 83.2 mmol) was added to the sodium ethoxide solution. After 30 min, bromoethane (15.0 mL, 21.9 g, 201 mmol) was added dropwise via an addition funnel and the funnel was washed with absolute ethanol (50 mL). The resultant solution was heated to reflux under argon for 18 h. Ethanol was removed *in vacuo* and diethyl ether (300 mL) was added to the residue. The white precipitate was removed by filtration and washed with diethyl ether (2 × 50 mL). The organic phases were combined and washed with sat aq sodium bicarbonate (400 mL) and brine (400 mL). The organic layer was dried over magnesium sulfate and filtered, and volatiles were removed *in vacuo*. The residue was crystallized from absolute ethanol at −20 °C, yielding 10.5 g (53.8 mmol, 65%) of **5b** as tan plates, R_f 0.44 (5% EtOAc/hexanes). ^{1}H NMR ($CDCl_3$) δ 1.24 (6H, t, $J = 7.0$ Hz), 2.02 (6H, s), 3.79 (4H, q, $J = 7.0$ Hz), 6.47 (2H, s); ^{13}C NMR ($CDCl_3$) δ 12.2, 15.1, 64.5, 109.4, 127.0, 151.1.

1,4-Bis-hexyloxy-2,3-dimethylbenzene (5d).[50] A solution of **4** (2.48 g, 18.0 mmol) in dry THF (35 mL) was slowly added *via* cannula to a suspension of sodium hydride (950 mg, 40 mmol) in THF (35 mL) under argon. The cannula was rinsed with THF (2 × 10 mL). Upon injection, an exothermic reaction was observed, and the resulting green colored solution was allowed to stir at room temperature. After 20 min, 1-iodohexane (5.3 mL, 7.6 g, 36 mmol) was added via syringe and the reaction mixture was heated to reflux for 72 h. The solution was cooled to room temperature, slowly quenched by addition of water (15 mL), and concentrated under a vacuum to a brown residue. The material was purified by flash chromatography (230–400 mesh silica) using hexanes as eluent to give 3.90 g (12.7 mmol, 71%) of **5d** as a yellow oil, R_f 0.73 (40% EtOAc/hexanes). IR (NaCl) cm^{-1} 1468, 1252; ^{1}H NMR (300 MHz, $CDCl_3$) δ 0.91 (6H, t, $J = 6.8$ Hz), 1.35 (8H, m), 1.48 (4H, pentet, $J = 7.2$ Hz), 1.77 (4H, pentet, $J = 6.8$ Hz), 2.17 (6H, s), 3.88 (4H, t, $J = 6.4$ Hz), 6.63 (2H, s); ^{13}C NMR (75 MHz, $CDCl_3$) δ 12.1, 14.0, 22.6, 25.8, 29.5, 31.6, 68.9, 109.1, 126.9, 151.2; HRMS (FAB+) calculated for $C_{20}H_{34}O_2$ (M^+) 306.2559, found 306.2563 (+1.2 ppm).

1-Bromo-2,5-bis-hexyloxy-3,4-dimethylbenzene (6d). A solution of bromine (1.6 mL, 5.0 g, 31 mmol) in $CHCl_3$ (75 mL) was added dropwise over a 30 min period to a solution of **5d** (8.92 g, 29.1 mmol) in $CHCl_3$ (75 mL) at room temperature under argon. After 45 min, the reaction mixture was diluted with CH_2Cl_2 (100 mL) and washed successively with sat aq $NaHCO_3$ (100 mL), sat aq Na_2SO_3 (100 mL), and brine (100 mL). The organic phase was dried ($MgSO_4$), filtered, and concentrated under a vacuum to give 10.1 g (26.2 mmol, 90%) of **6d** as a light yellow oil. IR (NaCl) cm^{-1} 1462, 1375, 1227, 1103; ^1H NMR (300 MHz, $CDCl_3$) δ 0.92 (6H, m), 1.35 (8H, m), 1.49 (4H, septet, J = 7.4 Hz), 1.79 (4H, septet, J = 7.1 Hz), 2.09 (3H, s), 2.22 (3H, s), 3.78 (2H, t, J = 6.6 Hz), 3.86 (2H, t, J = 6.5 Hz), 6.85 (1H, s); ^{13}C NMR (75 MHz, $CDCl_3$) δ 12.1, 13.4, 14.0, 14.1, 22.6, 22.6, 25.7, 25.8, 29.2, 30.1, 31.5, 31.7, 68.6, 73.2, 113.1, 113.5, 126.0, 132.3, 147.9, 153.4; HRMS (FAB+) calculated for $C_{20}H_{33}{}^{79}BrO_2$ (M^+) 384.1664, found 384.1672 (+2.1 ppm).

1-Bromo-3,4-bis-bromomethyl-2,5-bis-ethoxybenzene (7b). Compound **5b** (7.79 g, 40.1 mmol) was dissolved in dry CCl_4 (200 mL). NBS (14.3 g, 80.3 mmol) and benzoyl peroxide (BPO, 100 mg, 0.72 mmol, ~2 mol %) were added. The slurry was heated to reflux and stirred vigorously under argon. Additional BPO (100 mg) was added each hr. After 4.5 h ^1H NMR showed ring bromination in addition to side chain bromination. Additional NBS (7.14 g, 40.1 mmol) and BPO (100 mg) were added and the slurry was heated at reflux for 24 h. The slurry was cooled to room temperature and succinimide was removed by filtration. The organic phase was washed with aq sodium thiosulfate solution (100 mL), dried over magnesium sulfate, filtered, and concentrated *in vacuo*. The brown solid residue was crystallized from hexanes at −20 °C, yielding 11.8 g (27.4 mmol, 68%) of **7b** as a tan solid. ^1H NMR ($CDCl_3$) δ 1.43 (6H, m, J = 6.6 Hz), 3.91 (2H, q, J = 6.6 Hz), 4.05 (2H, q, J = 6.6 Hz), 4.60 (4H, s), 6.93 (1H, s).

1-Bromo-3,4-bis-bromomethyl-2,5-bis-hexyloxybenzene (7d). NBS (9.8 g, 55 mmol) was added in one portion to a solution of **6d** (10.1 g, 26.2 mmol) in CCl_4 (150 mL) under argon. A 250 W (115−125 V) IR heat lamp was positioned near the reaction flask to ensure a gentle reflux. After 24 h, the solution was cooled to room temperature, succinimide was removed by filtration, and the solid was washed with CCl_4 (20 mL). The solution was diluted with CH_2Cl_2 (100 mL) and washed successively with sat aq $NaHCO_3$ (100 mL), sat aq Na_2SO_3 (100 mL), and brine (100 mL). The organic phase was dried ($MgSO_4$), filtered, and concentrated under vacuum to give 14.0 g (25.8 mmol, 98%) of **7d** as a yellow oil. IR (NaCl) cm^{-1} 1455, 1245, 1011; ^1H NMR (300 MHz, $CDCl_3$) δ 0.91 (6H, m), 1.34 (8H, m), 1.48 (4H, m), 1.83 (4H, septet, J = 7.2 Hz), 3.95 (2H, t, J = 6.4 Hz), 4.02 (2H, t, J = 6.6 Hz), 4.69 (2H, s), 4.70 (2H, s), 7.02 (1H, s); ^{13}C NMR (75 MHz, $CDCl_3$) δ 14.0, 14.0, 22.6, 22.6, 23.5, 23.7, 25.5, 25.7, 29.0, 30.0, 31.4, 31.6, 69.0, 74.2, 117.1, 118.4, 125.8, 132.7, 148.6, 153.7; HRMS (FAB+) calculated for $C_{20}H_{31}{}^{79}Br_2{}^{81}BrO_2$ (M^+) 541.9855, found 541.9850 (−0.7 ppm).

Ethyl 2-Amino-4,7-diethoxyindan-2-carboxylate (9b). Ethyl 2-(benzylideneamino)acetate (8.32 g, 43.5 mmol) was dissolved in dry THF (1.8 L) and the solution was cooled to −78 °C under argon. Sodium hexamethyldisilazane (87 mL, 1 M in THF, 87 mmol) was added dropwise. After 30 min **7b** (15.0 g, 34.8 mmol) in THF (200 mL) was added dropwise. The reaction mixture was allowed to warm to room temperature and was stirred for 18 h. The reaction mixture was poured into brine (1 L) and the phases were separated. The aqueous phase was extracted with ethyl acetate (300 mL), the organic layers were combined, dried over anhydrous $MgSO_4$, filtered, and concentrated *in vacuo*. The resultant brown, viscous oil was dissolved in CH_2Cl_2 (200 mL) and passed through a plug of silica 60 (100 g) eluted with CH_2Cl_2, yielding 9.5 g of crude **8b** as a brown paste that was directly hydrogenated. The paste was dissolved in absolute ethanol (100 mL), 10% palladium on carbon (400 mg) was added, and the mixture was shaken for 48 h under H_2 (55 psi) on a Parr apparatus. Additional 10% palladium on carbon (1 g) was then added and the reaction was continued for 18 h. The mixture was passed through a plug of silica 60 (75 g) eluted with CH_2Cl_2 (500 mL) and volatiles were removed *in vacuo*. The brown residue was loaded onto a plug of silica 60 (100 g) using CH_2Cl_2, the plug was eluted with 10% methanol in CH_2Cl_2 (1 L), and the eluent was concentrated *in vacuo*. The residue was dissolved in CH_2Cl_2 (300 mL), and the solution was washed with sat. aq. sodium bicarbonate solution (200 mL), dried over $MgSO_4$, filtered, and concentrated *in vacuo*. The residue was subjected to flash chromatography on silica 60 (400 mL) using a gradient of 2.5−5% methanol in 1/1 EtOAc/hexanes, yielding 4.06 g (13.8 mmol, 40%) of **9b** as a viscous brown oil. ^1H NMR ($CDCl_3$) δ 1.28 (3H, t, J = 7.5 Hz), 1.37 (6H, t, J = 6.9 Hz), 1.78 (2H, bs), 2.92 (2H, d, J = 16.2 Hz), 3.46 (2H, d, J = 16.2 Hz), 3.98 (2H, q, J = 7.2 Hz), 4.21 (4H, q, J = 7.2 Hz), 6.62 (2H, s); ^{13}C NMR ($CDCl_3$) δ 14.2, 15.0, 43.8, 61.2, 63.9, 64.6, 110.5, 130.1, 149.6, 176.7; HRMS (FAB) calculated for $C_{16}H_{23}O_4N$ 294.1705, found 294.1712.

Ethyl 2-Amino-4,7-bis-hexyloxyindan-2-carboxylate (9d). Dry acetonitrile (850 mL) was added in one portion to a flask containing **7d** (14.2 g, 26.1 mmol), tetrabutylammonium iodide (1.9 g, 5.1 mmol), and finely ground potassium carbonate (43 g, 311 mmol) under argon. The slurry was stirred and heated to reflux in an oil bath at 85−90 °C. Ethyl isocyanoacetate (3.1 mL, 3.2 g, 28 mmol) was injected. Vigorous stirring was essential for an efficient and complete reaction. After 15 h, the solution was cooled to room temperature and filtered, and the salts were washed thoroughly with CH_2Cl_2. The organic phase was concentrated under a vacuum to a brown residue. Flash chromatography (230−400 mesh silica) using 10% EtOAc/hexanes as eluent produced 9.0 g of crude **10d** as a yellow oil, R_f 0.38 (10% EtOAc/hexanes). The crude isocyanate was dissolved in a mixture of absolute EtOH (80 mL) and conc. HCl (5 mL) and the solution was stirred overnight at room temperature. The volatiles were removed under a vacuum to leave a white solid. The solid was taken up in water (250 mL), the solution was basified with conc. NH_4OH, and extracted with Et_2O (3 × 200 mL). The organic extracts were combined, dried ($MgSO_4$), filtered, and concentrated under a vacuum to produce a yellow residue. The material was subjected to flash column chromatography (230−400 mesh silica, pretreated with 1% NEt_3) using 10% EtOAc/hexanes as eluent until all yellow nonpolar impurities were removed. The eluent was then changed to 30% EtOAc/hexanes, affording 5.0 g of crude **11d** as a brown oil, R_f 0.29 (30% EtOAc/hexanes). The crude amine **11d** was dissolved in absolute EtOH (50 mL), 10% Pd/C (2.4 g) was added, and the compound was hydrogenolyzed using a Parr apparatus (H_2 gas at 55 psi). Additional 10% Pd/C (100 mg) was added to the reaction each day. After 4 days, the reaction mixture was filtered, the catalyst was washed with CH_2Cl_2, and the filtrate was concentrated under a vacuum to leave an orange residue. Gravity column chromatography (silica gel 60 eluted with 40% EtOAc/hexanes, column pretreated with 1% NEt_3) gave 1.97 g (4.9 mmol, 19% for 3 steps) of **9d** as a yellow oily solid, R_f 0.48 (50% EtOAc/hexanes), mp 35−36 °C. IR (KBr) cm^{-1} 1727; ^1H NMR (200 MHz, $CDCl_3$) δ 0.87 (6H, t, J = 6.6 Hz), 1.13 (15H, m), 1.71 (6H, m), 2.88 (2H, d, J = 16.4 Hz), 3.42 (2H, d, J = 16.4 Hz), 3.86 (4H, dt, J = 2.2, 6.4 Hz), 4.18 (2H, q, J = 7.2 Hz), 6.58 (2H, s); ^{13}C NMR (50 MHz, $CDCl_3$) δ 13.9, 14.1, 22.5, 25.6, 29.7, 31.5, 43.8, 61.1, 64.6, 68.3, 110.4, 130.1, 149.8, 176.7; HRMS (FAB+) calculated for $C_{24}H_{40}NO_4$ $(M + H)^+$ 406.2957, found 406.2952 (−1.3 ppm).

Ethyl 2-*tert*-Butoxycarbonylamino-4,7-diethoxyindan-2-carboxylate (12b). Amino ester **9b** (3.00 g, 10.2 mmol) and di-*tert*-butyl dicarbonate (2.45 g, 11.2 mmol) were dissolved in 50 mL of CH_2Cl_2. Triethylamine (2.0 mL, 1.4 g, 14 mmol) was added and the solution was allowed to stir at room temperature under argon for 18 h. Volatiles were removed *in vacuo* and the residue was crystallized from absolute ethanol, yielding 2.06 g (5.24 mmol, 51%) of **12b** as pale yellow crystals, R_f 0.45 (35% EtOAc/hexanes); ^1H NMR ($CDCl_3$) δ 1.24 (3H, t, J = 5.5 Hz), 1.36 (6H, t, J = 7.2 Hz), 1.42 (9H, s), 3.20 (2H, d, J = 17.0 Hz), 3.54 (2H, d, J = 17.0 Hz), 3.96 (4H, q, J = 6.6 Hz), 4.21 (2H, q, J = 6.9 Hz), 5.16 (1H, s), 6.61 (2H, s); ^{13}C NMR ($CDCl_3$) δ 14.1, 14.9, 28.2, 41.6, 61.4, 63.9, 65.6, 79.7, 110.7, 129.6, 149.35, 154.9, 173.5.

Anal. Calculated for $C_{21}H_{31}NO_6$: C, 64.10; H, 7.94, N, 3.56. Found: C, 64.15; H, 7.95, N, 3.74.

Ethyl 2-*tert*-Butoxycarbonylamino-4,7-bis-hexyloxyindan-2-carboxylate (12d). Di-*tert*-butyl dicarbonate (1.47 g, 6.74 mmol) was added to a solution of amino ester **9d** (1.81 g, 4.5 mmol) in a mixture of CH_2Cl_2 (25 mL) and brine (5 mL) and the reaction mixture was heated

Scheme 1. Synthesis of Tribromides 7b−h

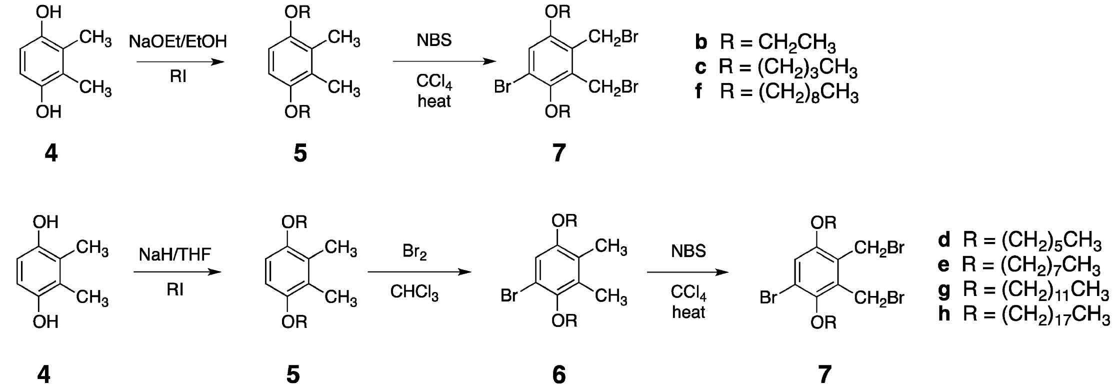

at a gentle reflux overnight. Additional di-*tert*-butyl dicarbonate (0.5 g, 2.3 mmol) was added to the solution after 24 h, and the reaction was heated at reflux an additional 6 h. The reaction mixture was diluted with CH_2Cl_2 (150 mL) and washed with brine (100 mL). The organic phase was dried ($MgSO_4$), filtered, and concentrated under a vacuum to give a yellow solid which was purified by flash chromatography (230−400 mesh silica, pretreated with 1% NEt_3) using 20% EtOAc/hexanes as eluent to obtain 1.99 g (3.93 mmol, 95%) of **12d** as an off-white solid, R_f 0.67 (30% EtOAc/hexanes), mp 63−64 °C. IR (KBr) cm^{-1} 3363 (b), 1733, 1709; ^1H NMR (300 MHz, $CDCl_3$) δ 0.87 (6H, t, J = 6.4 Hz), 1.20−1.40 (15H, m), 1.39 (9H, s), 1.50 (s, Boc_2O contaminant), 1.70 (4H, pentet, J = 6.8 Hz), 3.17 (2H, broad d, J = 17.1 Hz), 3.51 (2H, d, J = 16.8 Hz), 3.86 (4H, t, J = 6.4 Hz), 4.20 (2H, q, J = 7.1 Hz), 5.09 (1H, broad s), 6.58 (2H, s); ^{13}C (75 MHz, $CDCl_3$) δ 14.0, 14.1, 22.6, 25.7, 27.3 (Boc_2O contaminant), 28.1, 29.3, 31.5, 41.5, 61.4, 65.7, 68.4, 79.8, 85.1 (Boc_2O contaminant), 110.5, 129.6, 146.7 (Boc_2O contaminant), 149.5, 154.8, 173.5; HRMS (FAB+) calculated for $C_{29}H_{47}NO_6$ (M^+) 505.3403, found 505.3403 (−0.1 ppm).

Anal. Calculated for $C_{29}H_{47}NO_6$: C, 68.88; H, 9.37, N, 2.77 Found: C, 68.82; H, 9.48, N, 3.06.

2-*tert*-Butoxycarbonylamino-4,7-diethoxyindan-2-carboxylic Acid (13b). Ester **12b** (1.00 g, 2.54 mmol) was dissolved in ethanol (25 mL). Distilled water (10 mL) and potassium hydroxide (1.00 g, 17.8 mmol) were added. The mixture was stirred under argon for 18 h and then diluted to 150 mL with distilled H_2O and acidified with 2 N HCl. The mixture was extracted with ether (2 × 150 mL), the organic layers were combined, dried over anhydrous Na_2SO_4, filtered, and volatiles were removed *in vacuo* to give 859 mg (2.35 mmol, 92%) of **13b** as a tan foam, R_f 0.10 (20% EtOAc/hexanes). ^1H NMR ($CDCl_3$) δ 1.36 (6H, t, J = 6.9 Hz), 1.41 (9H, s), 3.24 (2H, d, J = 15.3 Hz), 3.60 (2H, d, J = 17.1 Hz), 3.97 (4H, q, J = 6.9 Hz), 5.22 (1H, s), 6.61 (2H, s), 10.5 (1H, s); ^{13}C NMR ($CDCl_3$) δ 15.0, 28.2, 41.4, 64.0, 65.4, 80.4, 110.7, 129.5, 149.3, 155.5, 178.4.

Anal. Calculated for $C_{19}H_{27}NO_6$: C, 62.45; H, 7.45, N, 3.83 Found: C, 62.54; H, 7.68, N, 3.97.

2-*tert*-Butoxycarbonylamino-4,7-bis-hexyloxyindan-2-carboxylic Acid (13d). Potassium hydroxide (2.0 g, 30 mmol) was added to a solution of ester **12d** (1.83 g, 3.62 mmol) in absolute EtOH (60 mL) followed by addition of water (15 mL). The solution gradually went from opaque to a clear yellow solution upon heating to a gentle reflux. After 1 h, the reaction mixture was cooled to room temperature and the solvent was removed under a vacuum to leave a white solid. The solid was dissolved in water (100 mL) and the solution was acidified with conc. HCl to a pH of 2. The aqueous solution was extracted with EtOAc (3 × 100 mL), and the organic phases were combined, washed with brine (100 mL), dried ($MgSO_4$), filtered, and concentrated under a vacuum to give 1.57 g (3.29 mmol, 91%) of **13d** as an off-white solid, R_f 0.56 (20% EtOAc/hexanes), mp 116 °C. IR (KBr) cm^{-1} 3351, 3086, 1746, 1672; ^1H NMR (300 MHz, $CDCl_3$) δ 0.88 (6H, t, J = 6.5 Hz), 1.20−1.50 (21H, m), 1.72 (4H, pentet, J = 6.8 Hz), 3.22 (2H, broad d, J = 15.4 Hz), 3.58 (2H, d, J = 16.9 Hz), 3.87 (4H, t, J = 6.5 Hz), 5.18 (1H, s), 6.58 (2H, s), 11.87 (1H, s); ^{13}C NMR (75 MHz, $CDCl_3$) δ 14.0, 22.6, 25.7, 28.2, 29.3, 31.6, 41.4, 65.4, 68.5, 80.3, 110.6, 129.5, 149.5, 155.4, 178.8; HRMS (FAB+) calcd for $C_{27}H_{43}NO_6$ (M^+) 477.3090, found 477.3089 (−0.3 ppm).

Ethyl 2-[(2-*tert*-Butoxycarbonylamino-4,7-diethoxyindane-2-carbonyl)amino]-4,7-diethoxyindan-2-carboxylate (14b). Acid **13b** (150 mg, 0.410 mmol) and amine **9b** (120 mg, 0.410 mmol) were dissolved in DMF (5 mL). Triethylamine (150 μL, 109 mg, 1.07 mmol) was added via syringe. BOP reagent (181 mg, 0.410 mmol) was added and the mixture was stirred under argon for 72 h. The mixture was then diluted with EtOAc (150 mL) and washed with brine (2 × 200 mL). The organic phase was dried over $MgSO_4$, filtered, and volatiles were removed *in vacuo*. The residue was dissolved in CH_2Cl_2 (25 mL) and decolorizing charcoal (2 g) was added. After stirring at room temperature for 48 h the charcoal was removed by filtration and volatiles were removed, yielding 244 mg (0.381 mmol, 93%) of **14b** as a tan solid, R_f 0.81 (30% EtOAc/hexanes), 0.58 (20% EtOAc/hexanes). ^1H NMR δ 1.21 (12H, t, J = 6.3 Hz), 1.32 (9H, s), 1.34 (3H, t, J = 6.5 Hz), 2.92 (1H, s), 3.27 (4H, bd, J = 13.2 Hz), 3.57 (4H, d, J = 16.8 Hz), 3.94 (8H, m), 4.17 (2H, q, J = 6.6 Hz), 6.60 (4H, s), 7.19 (1H, s); ^{13}C NMR ($CDCl_3$) δ 14.0, 14.9, 28.0, 40.4, 41.3, 61.4, 63.9, 110.6, 129.7, 149.3, 149.5, 154.7, 172.9.

Anal. Calculated for $C_{35}H_{48}N_2O_9$: C, 65.61; H, 7.55, N, 4.37 Found: C, 65.74; H, 7.51, N, 4.46.

Ethyl 2-[(2-*tert*-Butoxycarbonylamino-4,7-bis-hexyloxyindane-2-carbonyl)amino]-4,7-bis-hexyloxyindan-2-carboxylate (14d). A procedure similar to that used in the synthesis of **14b** employing acid **13d** (537 mg, 1.12 mmol), amine **9d** (434 mg, 1.07 mmol), triethylamine (300 μL, 218 mg, 2.14 mmol), and BOP reagent (473 mg, 1.07 mmol) in DMF (5 mL) gave a residue which was chromatographed on silica 60 (250 mL) using 10% EtOAc/hexanes as eluent. The product so obtained was crystallized from absolute ethanol, yielding 347 mg of **14d** as an off-white solid. The mother liquor was concentrated in vacuo and the residue was chromatographed on silica 60 (150 mL) using ether as the eluent. The product so obtained was crystallized from absolute ethanol, yielding an additional 134 mg of **14d** for a total yield of 481 mg (0.556 mmol, 52%), R_f 0.60 (30% EtOAc/hexanes). ^1H NMR ($CDCl_3$) δ 0.90 (12H, m), 1.23−1.42 (36H, m), 1.71 (8H, m), 3.00 (1H, s), 3.23 (4H, d, J = 16.5 Hz), 3.58 (4H, d, J = 17.1 Hz), 3.85 (8H, t, J = 6.5 Hz), 4.18 (2H, q, J = 7.2 Hz), 5.20 (1H, s), 6.56 (2H, s), 6.59 (2H, s); ^{13}C NMR ($CDCl_3$) δ 14.1, 22.6, 25.6, 25.7, 25.8, 28.0, 29.3, 29.4, 31.5, 31.6, 41.4, 61.4, 68.5, 110.7, 129.7, 149.5, 149.7, 154.7, 172.9.

Anal. Calculated for $C_{51}H_{80}N_2O_9$: C, 70.80; H, 9.32, N, 3.24 Found: C, 70.72; H, 9.51, N, 3.33.

***cyclo*-Bis-(2-amino-4,7-diethoxyindan-2-carboxylic Acid) (3b).** A glass tube containing **14b** (152 mg, 0.237 mmol) was evacuated to ~1 mmHg and sealed using an O_2/methane torch. The tube was heated to 250 °C in an oil bath for 15 min where melting, outgassing, and recrystallization were observed. The resulting residue was insoluble in CH_2Cl_2, butanol, or THF, but dissolved in hot DMSO (100 mL). Decolorizing charcoal (2 g) was added, and the slurry was heated for 1 h with stirring. The charcoal was removed by filtration and the hot solution was diluted with 500 mL of brine. The brine/DMSO mixture

Scheme 2. Synthesis of Amino Esters 9b–h

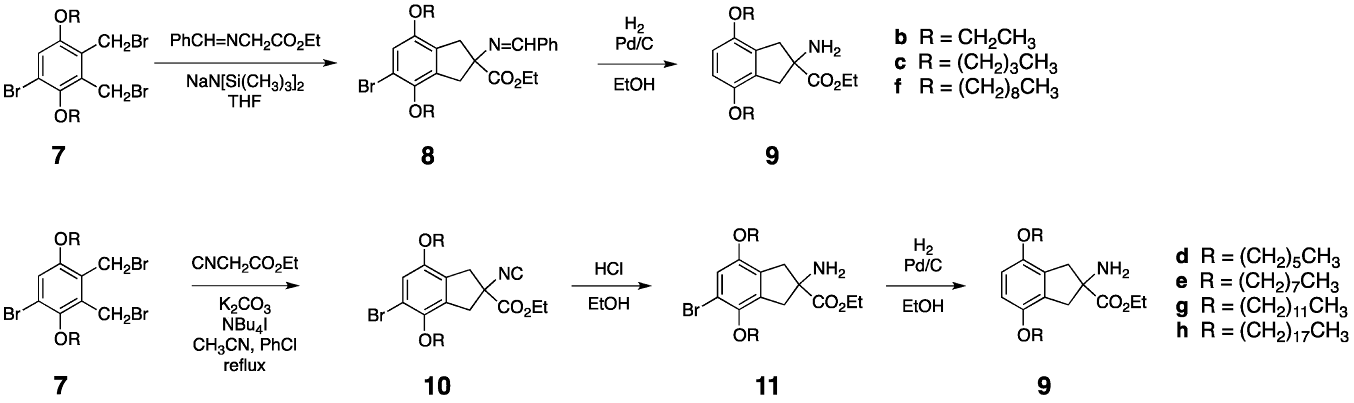

Scheme 3. Synthesis of Compounds 3b–3h

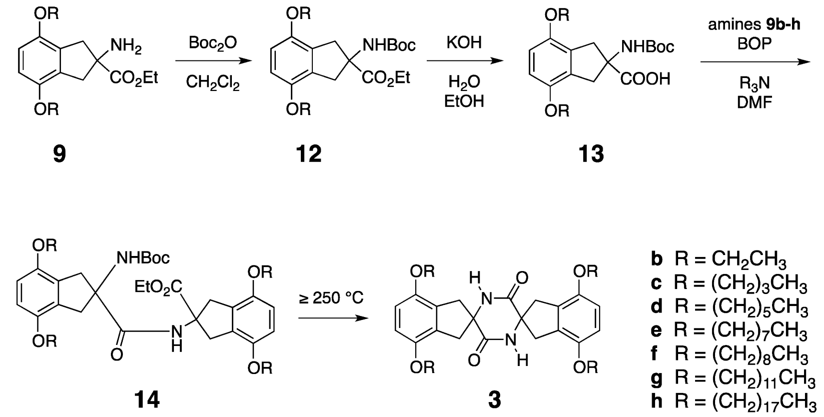

was extracted with THF (2 × 250 mL). The organic layers were combined, dried over anhydrous $MgSO_4$, and concentrated *in vacuo*. The decolorizing procedure was repeated, and the residue washed with methanol (2 × 10 mL). Slow recrystallization of the residue from hot DMSO then yielded 72 mg (0.15 mmol, 61%) of **3b** as white blocks. ^1H NMR (TFA-*d*) 1.37 (12H, t, $J = 6.75$ Hz), 3.43 (4H, d, $J = 17$ Hz), 3.86 (4H, d, $J = 17$ Hz), 4.19 (8H, q, $J = 6.7$ Hz), 6.92 (4H, s); ^{13}C NMR (TFA-*d*) 15.4, 46.4, 68.8, 70.2, 119.0, 131.7, 151.6, 174.6.

Anal. Calculated for $C_{28}H_{34}N_2O_6$: C, 68.00; H, 6.93, N, 5.66 Found: C, 68.07; H, 7.04, N, 5.78.

***cyclo*-Bis-(2-amino-4,7-*bis*-hexyloxyindan-2-carboxylic Acid) (3d).** A glass tube containing **14d** (251 mg, 0.290 mmol) was evacuated to ~1 mmHg and sealed using an O_2/methane torch. The tube was heated to 250 °C in an oil bath for 40 min where melting and outgassing were observed. The oily residue solidified upon cooling to room temperature. Recrystallization of the residue from absolute ethanol yielded 163 mg (0.227 mmol, 78%) of **3d** as white needles. ^1H NMR ($CDCl_3$) δ 0.91 (12H, t, $J = 6.3$ Hz), 1.35–1.45 (24H, m), 1.76 (8H, m), 3.17 (4H, d, $J = 16.5$ Hz), 3.71 (4H, d, $J = 16.2$ Hz), 3.91 (8H, t, $J = 6.3$ Hz), 6.37 (2H, s), 6.65 (4H, s); ^{13}C NMR ($CDCl_3$) δ 14.1, 22.6, 25.7, 29.3, 31.6, 44.6, 66.7, 68.5, 111.1, 128.0, 149.7, 169.3.

Anal. Calculated for $C_{44}H_{66}N_2O_6$: C, 73.50; H, 9.25, N, 3.90 Found: C, 73.75; H, 9.25, N, 4.05.

Table 1. Crystallographic Data for Piperazinediones 3b, 3c, and 3g

	3b	3c	3g
formula	$C_{28}H_{34}N_2O_6$	$C_{36}H_{50}N_2O_6$	$C_{68}H_{114}N_2O_6$
weight (g mol^{-1})	494.57	606.78	1055.61
temp (K)	170(2)	170(2)	100(2)
radiation	Mo Kα	Mo Kα	synchrotron
cryst syst	monoclinic	monoclinic	monoclinic
space group	$P2_1/n$	$P2_1/n$	$P2_1/c$
a (Å)	9.8429(13)	14.6172(19)	21.981(4)
b (Å)	6.1190(8)	6.0380(8)	18.298(4)
c (Å)	21.635(3)	19.251(3)	24.801(5)
α (deg)	90	90	90
β (deg)	91.328(2)	92.895(3)	108.72(3)
γ (deg)	90	90	90
V (Å^3)	1302.7(3)	4474(2)	9447(3)
Z	2	2	6
R_1 (obs data)	0.0423	0.0503	0.0992
wR_2 (all data)	0.1049	0.1364	0.2971
GOF on F^2	1.047	1.030	1.098

■ RESULTS

Synthesis of Compounds 3b–3h. Compounds **3b–3h** were prepared as depicted in Schemes 1–3 and in a manner analogous with the published synthesis of **3a.**[44] Commercially available 2,3-dimethylhydroquinone[51] (**4**) was deprotonated (NaOEt/EtOH or NaH/THF) and alkylated using normal alkyl iodides of varying chain lengths, producing compounds **5b–5h** (Scheme 1). Yields ranged from 45 to 78%. In ethanol, yields were generally lower and byproducts from ring alkylation became more pronounced for the longer chain iodides, so THF was the preferred solvent for these reactions. Direct tribromination of **5b**, **5c**, and **5f** in CCl_4 using NBS under free radical conditions led to **7b**, **7c**, and **7f** in yields of 68%, 62%, and 33%, respectively. These halogenation reactions were particularly sluggish, and so for **5d**, **5e**, **5g**, and **5h** ionic nuclear monobromination (Br_2, $CHCl_3$) was carried out prior to side chain bromination under free radical

Table 2. Conformational Data for Piperazinediones 3a–3c and 3g[a]

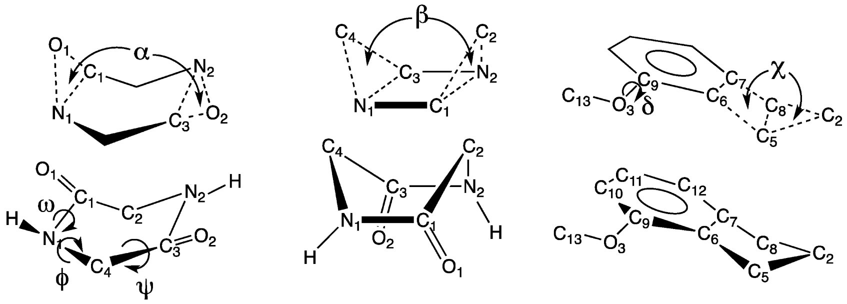

compound	conformer	ϕ^b	ψ^b	ω^b	α^c	β^c	χ^d	δ^e	chain
3a[f]	A	−10.3	8.0	4.7	173	165	146	172	a
		−12.1	6.4	2.8			145	−165	b
								165	c
								−173	d
3b	B	2.2	2.0	2.3	180	180	145	176	a
		−2.2	−2.0	−2.3			145	−174	b
								174	c
								−176	d
3c	C	0.5	0.5	0.5	180	180	146	176	a
		−0.5	−0.5	−0.5			146	−175	b
								175	c
								−176	d
3g	G_1	13.0	−4.8	5.5	173	165	148	157	a
		3.9	−13.0	−4.1			144	−164	b
								169	c
								−177	d
	G_2	13.0	−4.8	5.5	173	165	150	168	a
		3.9	−13.0	−4.1			148	−177	b
								−169	c
								−174	d
	G_3	0.3	0.3	0.3	180	180	147	173	a
		−0.3	−0.3	−0.3			147	−161	b
								161	c
								−173	d
	G_4	0.3	0.3	0.3	180	180	147	174	a
		−0.3	−0.3	−0.3			147	−173	b
								173	c
								−174	d

[a] Values are in degrees and are given for each substructural component. [b] The dihedral angles ϕ, ψ, and ω are the torsion angles defined for conformational analysis of amide bonds in peptides (see ref 56). [c] The dihedral angles α and β were previously defined (see ref 12) and are measures of the degree of nonplanarity of the piperazinedione ring (for flat rings $\alpha = \beta = 180°$). [d] The dihedral χ was previously defined (see ref 44) and is a measure of the degree of nonplanarity of the cyclopentene ring component of the indane system (for flat rings $\chi = 180°$). [e] The C_6–C_9–O_3–C_{13} torsion angle, δ, measures the twist of the alkoxy substituent relative to the plane of the benzene ring. [f] Data taken from ref 44.

conditions (NBS, CCl_4).[52] The yields to **7d**, **7e**, **7g**, and **7h** via **6d**, **6e**, **6g**, and **6h** were 88%, 90%, 96%, and 85%, respectively, over the two steps.

Condensation of tribromides **7b**, **7c**, and **7f** with ethyl 2-(benzylideneamino)acetate by the method of Kotha and Kuki[53] gave indanone derivatives **8b**, **8c**, and **8f** (Scheme 2). Hydrogenolysis of the imine and carbon–bromine bonds (10% Pd/C, H_2 @ 55 psi, EtOH) gave the amino esters **9b**, **9c**, and **9f** in 40%, 43%, and 36% yields, respectively, over two steps. Condensation of tribromides **7d**, **7e**, **7g**, and **7h** with ethyl isocyanoacetate by the method of Kotha and Brahmachany[54] gave indanone derivatives **10d**, **10e**, **10g**, and **10h**. Hydrolysis of the isonitrile functionality (aq HCl, EtOH) produced the corresponding amino esters **11d**, **11e**, **11g**, and **11h**. Hydrogenolysis of the carbon–bromine bonds (10% Pd/C, H_2 @ 55 psi, EtOH) gave the corresponding amino esters **9d**, **9e**, **9g**, and **9h** in 19%, 24%, 46%, and 33% yields, respectively, over three steps.

Amino esters **9b**–**9h** were converted to the corresponding *N*-Boc esters **12b**–**12h** in yields typically ranging from 50 to 60% (Scheme 3). Esters **12b**–**12h** were then saponified to give *N*-Boc acids **13b**–**13h** in yields typically ranging from 85 to 95%. Couplings of amino esters **9b**–**9h** with the corresponding *N*-Boc acids **13b**–**13h** were effected using (benzotriazol-1-yloxy)tris-(dimethylamino)phosphonium hexafluorophosphate[53,55] (BOP reagent) and a tertiary amine base (Et_3N or DABCO) in DMF at room temperature, affording the dipeptides **14b**–**14h** in yields typically ranging from 45 to 75%. Thermolysis of these dipeptides (neat under vacuum, ca. 250 °C) produced the corresponding piperazinediones **3b**–**3h** in yields ranging from 60 to 78%.

Crystal Structures. NMR spectra of compounds **3b**–**3h** were consistent with the expected C_{2h} point group symmetry for

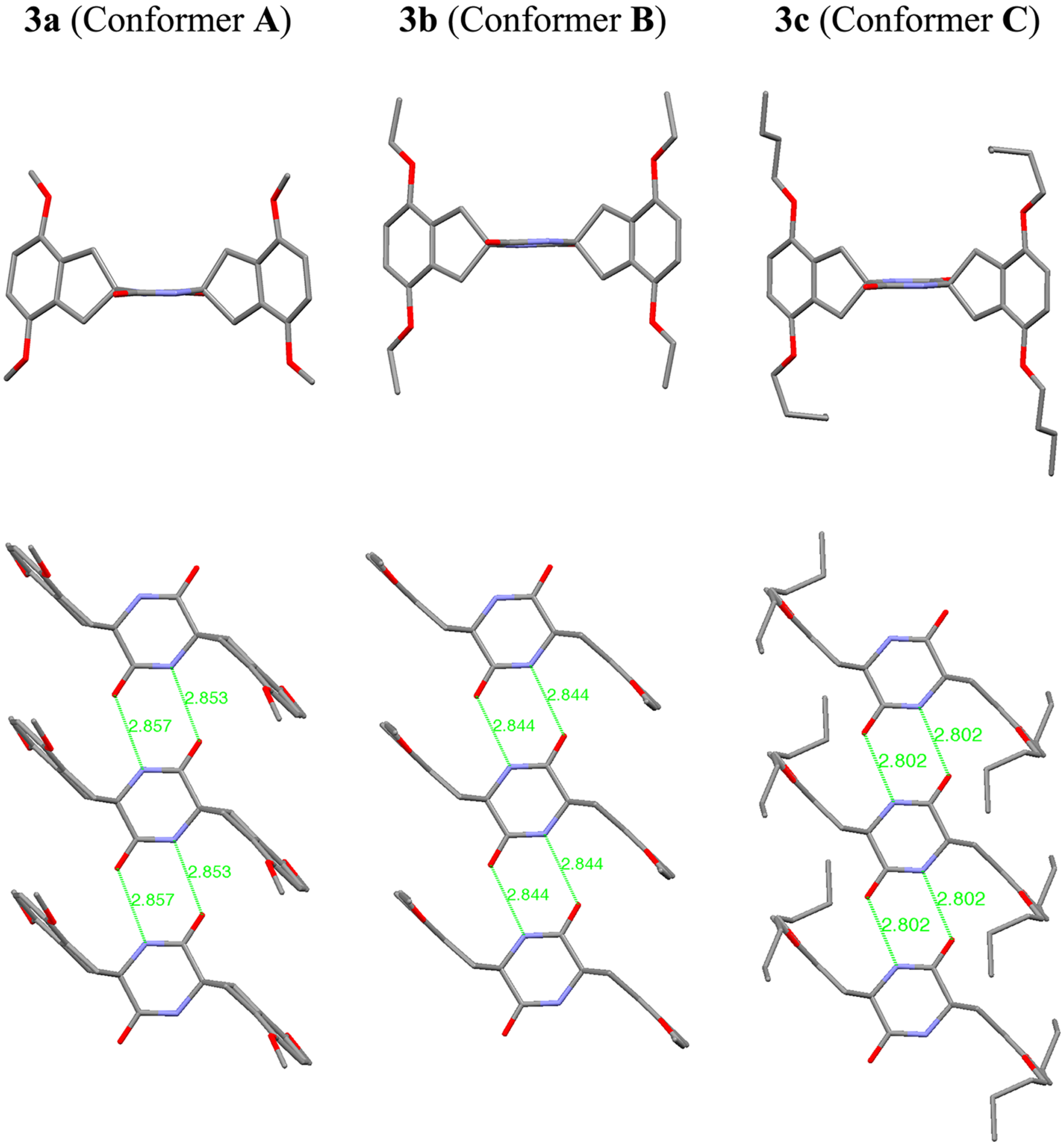

Figure 3. Two views of hydrogen-bonded 1D-tapes from the crystal structures of compounds **3a**−**3c**. Top: A view parallel to the long axis of the tape. Bottom: A view perpendicular to the long axis of the tape. These views serve to illustrate the conformations **A**−**C** of the piperazinediones observed in the crystals.

these molecules in solution. Crystal structure data for compounds **3b**, **3c**, and **3g** are given in Table 1. Geometric data for the conformers resident in the crystals are given in Table 2.[56]

Previously it was observed that compound **3a** crystallized from hot DMSO in space group $C2$.[44] One conformer (see Figure 3, conformer **A**) possessing C_1 symmetry was present in the crystal. The piperazinedione ring of **A** adopted a shallow pseudoboat conformation (see Table 2, $\alpha_{\mathbf{A}} = 173°$, $\beta_{\mathbf{A}} = 165°$) and the cyclopentene subunits of the indane rings were substantially bent toward the proximal nitrogen in the piperazinedione ring ($\chi_{\mathbf{A}} = 145°$, 146°). The carbon atoms of the four methyl ether groups were directed away from the piperazinedione core. Two were only slightly torsionally displaced from the average planes defined by the arenes to which they were attached ($\delta_{\mathbf{A}} = 172°$, $-173°$) and two were more substantially displaced ($\delta_{\mathbf{A}} = 165°$, $-165°$). Nevertheless, 2-fold rotational symmetry very nearly exists for conformer **A**.

In the present study, compound **3b** crystallized from hot DMSO in space group $P2_1/n$. One conformer (Figure 3, **B**) possessing C_i symmetry was present in the crystal. The piperazinedione ring of **B** adopts a flat conformation ($\alpha_{\mathbf{B}} = 180°$, $\beta_{\mathbf{B}} = 180°$) and the cyclopentene subunits of the indane rings are substantially bent toward the proximal nitrogen in the piperazinedione ring ($\chi_{\mathbf{B}} = 145°$, 145°). In this case, all the carbon atoms of the ethyl ether groups are only slightly torsionally displaced from the average planes defined by the arenes to which they are attached. The methylene carbons point away from the piperazinedione core ($174° \leq |\delta| \leq 176°$), while the methyl carbons point back toward the piperazinedione core.

Compound **3c** crystallized from hot absolute ethanol in space group $P2_1/n$. One conformer (Figure 3, **C**) possessing C_i symmetry was present in the crystal. The piperazinedione ring of **C** adopts a flat conformation ($\alpha_{\mathbf{C}} = 180°$, $\beta_{\mathbf{C}} = 180°$) and the cyclopentene subunits of the indane rings are substantially bent

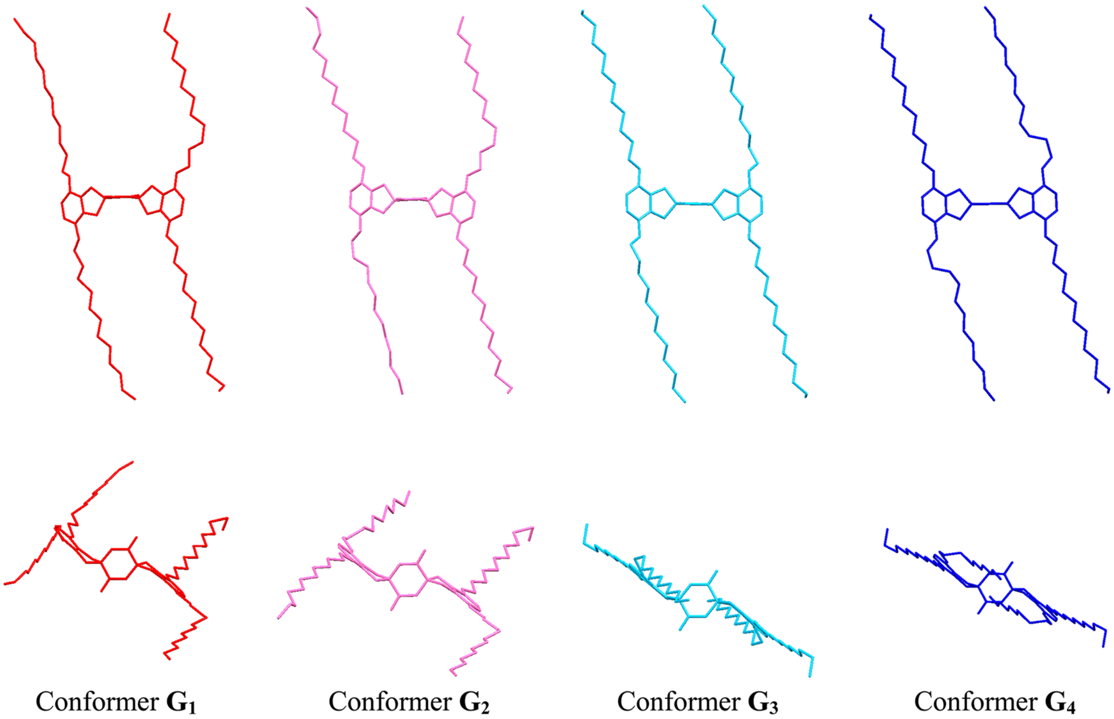

Figure 4. Two views of conformers $\mathbf{G_1}$-$\mathbf{G_4}$ found in the crystal structure of **3g**. In these depictions, conformer $\mathbf{G_1}$ is red, $\mathbf{G_2}$ is lavender, $\mathbf{G_3}$ is light blue, and $\mathbf{G_4}$ is dark blue. Top: A view parallel to the long axis of the hydrogen-bonded tape. Bottom: A view perpendicular to the long axis of the hydrogen-bonded tape.

Table 3. Intermolecular Structural Parameters for Self-Association of Piperazinediones 3a−3c and 3g: Hydrogen Bonding[a]

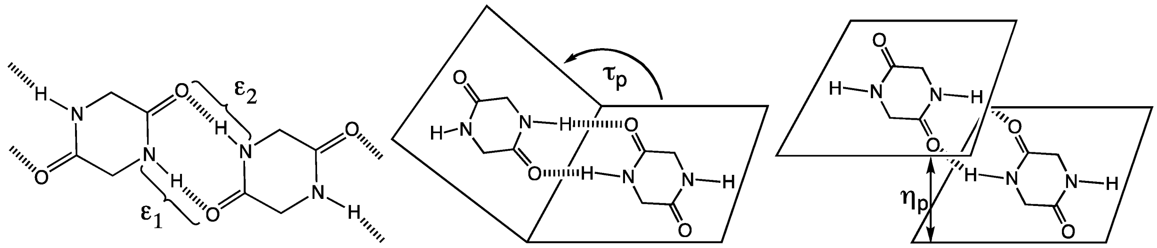

compound	N−O distances ε_1 (Å)[b]	N−O distances ε_2 (Å)[b]	τ_p (deg)[c]	η_p (Å)[d]
3a[e]	2.85	2.86	0.0	0.04
3b	2.84	2.84	0.0	0.23
3c	2.80	2.80	0.0	0.40
3g[f]	2.88	2.88	0.0	0.37
3g[g]	2.82	2.91	21.3	na[h]
CSD average	2.88		0.0	0.29

[a] Values are listed for each substructural component. [b] The distances ε_1 and ε_2 lie between the amide nitrogen and oxygen atoms involved in hydrogen bonding. [c] The dihedral angle τ_p is formed by the intersection of the average planes defined by the atoms of adjacent piperazinedione rings in a tape. [d] The distance η_p lies between parallel average planes defined by the atoms of adjacent piperazinedione rings in a tape. [e] Data taken from ref 44. [f] Interactions of conformers A and B with conformers A and B. [g] Interactions of conformers A and B with conformers C and D. [h] Not applicable.

toward the proximal nitrogen in the piperazinedione ring (χ_C = 146°, 146°). Two out of four butoxy chains are related by inversion symmetry and are present in g_+g_+ and g_-g_- "pentane" conformations (including the oxygen). The other two butoxy chains contain a single g_+ or g_- twist about the $ArOCH_2$−$CH_2CH_2CH_3$ σ bond. As was the case for conformers **A** and **B**, the methylene carbons adjacent to the ether oxygen point away from the piperazinedione core and are only slightly torsionally displaced from the average planes defined by the arenes to which they are attached ($175° \leq |\delta| \leq 176°$). However, the remaining carbon atoms of the butoxy chains project further and further from these planes. The carbon-to-arene plane distances proceeding from the ether oxygen are 0.12, 0.40, 1.86, and 2.87 Å for the butoxy chains with two gauche twists and 0.07, 0.10, 1.45, and 1.64 Å for the chains with a single gauche twist.

Attempts to analyze crystals of **3d**, **3e**, and **3f** by single crystal X-ray analysis were unsuccessful. Crystals could be grown from hot absolute ethanol as white needles, but were too weakly diffracting to be of use. Fortunately, compound **3g** crystallized from isopropanol in space group $P2_1/c$ and a structure was

Table 4. Intermolecular Structural Parameters for Self-Association of Piperazinediones 3a−3c and 3g: Arene Interactions[a]

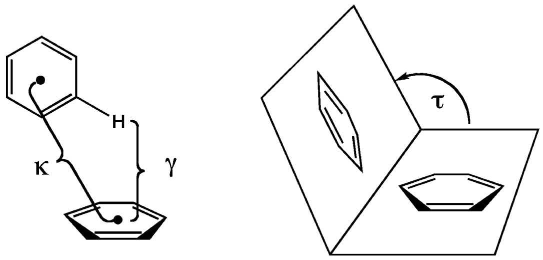

	arene centroid-to-centroid distances (κ), angles between arene rings (τ), and centroid-to-closest arene hydrogen distances (γ) on each tape edge[a,b]					
compound	κ_1 (Å)	κ_2 (Å)	τ_1 (deg)	τ_2 (deg)	γ_1 (Å)	γ_2 (Å)
3a[c]	4.90	5.56	86.3	85.6	2.76	3.26[d]
3b	4.89	4.89	82.9	82.9	2.68	2.68
3c	5.77	5.77	84.2	84.2	3.53[e]	3.53[e]
3g[f]	4.89	4.89	88.6	88.6	2.79	2.79
3g[g]	4.80	5.41	89.4	86.6	2.87	3.10

[a] Values are listed for each substructural component. [b] For optimal perpendicular edge-to-center interactions, $\kappa \approx 5.0$ Å and $\tau \approx 90°$ (see refs 57−60). [c] Data taken from ref 44. [d] On this tape edge methoxy hydrogens are located 3.02 Å and 3.29 Å from the arene centroid. [e] Butoxy hydrogens ($\text{Ar-OC}\underline{\text{H}}_2\text{Pr}$) are located 2.83 Å and 3.23 Å from the arene centroid. [f] Interactions of conformers A and B with conformers A and B. [g] Interactions of conformers A and B with conformers C and D.

determined using synchrotron radiation. Four conformers (Figure 4, $\mathbf{G_1}$-$\mathbf{G_4}$) were present in a 2:2:1:1 ratio in the crystal. Conformers $\mathbf{G_1}$ and $\mathbf{G_2}$ are similar in conformation and were coresident at a general position, while conformers $\mathbf{G_3}$ and $\mathbf{G_4}$ are similar in conformation and were coresident at a position with inversion of symmetry. The piperazinedione rings of $\mathbf{G_1}$ and $\mathbf{G_2}$ adopt unsymmetrical shallow boat conformations ($\alpha_{G1} = \alpha_{G2} = 173°$, $\beta_{G1} = \beta_{G2} = 165°$) and the cyclopentene subunits of the indane rings are substantially bent toward the proximal nitrogen in the piperazinedione ring ($\chi_{G1} = 148°, 144°$ and $\chi_{G2} = 150°, 148°$). The piperazinedione rings of $\mathbf{G_3}$ and $\mathbf{G_4}$ are flat ($\alpha_{G1} = \alpha_{G2} = 180°$, $\beta_{G1} = \beta_{G2} = 180°$) and the cyclopentene subunits of the indane rings are substantially bent toward the proximal nitrogen in the piperazinedione ring ($\chi_{G1} = \chi_{G2} = 147°, 147°$). In all cases the methylene carbons adjacent to the ether oxygen point away from the piperazinedione core and are slightly to moderately torsionally displaced from the average planes defined by the arenes to which they are attached ($157° \leq |\delta| \leq 174°$). While the dodecyloxy chains exhibit predominantly extended (antiperiplanar) conformations, there are significant deviations from an extended conformation in the following positions: $\mathbf{G_{1a}}$ −68° ($OC_1{-}C_2C_3$), $\mathbf{G_{1b}}$ 138° ($C_1C_2{-}C_3C_4$) and 127° ($C_2C_3{-}C_4C_5$), $\mathbf{G_{1c}}$ 88° ($C_9C_{10}{-}C_{11}C_{12}$), $\mathbf{G_{1d}}$ 61° ($C_2C_3{-}C_4C_5$); $\mathbf{G_{2a}}$ 88° ($C_9C_{10}{-}C_{11}C_{12}$), $\mathbf{G_{2b}}$ 61° ($C_2C_3{-}C_4C_5$), $\mathbf{G_{2c}}$ 87° ($OC_1{-}C_2C_3$), $\mathbf{G_{2d}}$ −158° ($OC_1{-}C_2C_3$) and 112° ($C_9C_{10}{-}C_{11}C_{12}$); $\mathbf{G_{3a}}$ −75° ($C_9C_{10}{-}C_{11}C_{12}$), $\mathbf{G_{3b}}$ 153° ($C_{Ar}O{-}C_1C_2$) and 68° ($OC_1{-}C_2C_3$), $\mathbf{G_{3c}}$ −153° ($C_{Ar}O{-}C_1C_2$) and −68° ($OC_1{-}C_2C_3$), $\mathbf{G_{3d}}$ 75° ($C_9C_{10}{-}C_{11}C_{12}$); $\mathbf{G_{4a}}$ 63° ($OC_1{-}C_2C_3$) and −154 ($C_1C_2{-}C_3C_4$), $\mathbf{G_{4b}}$ 75° ($C_9C_{10}{-}C_{11}C_{12}$), $\mathbf{G_{4c}}$ −75° ($C_9C_{10}{-}C_{11}C_{12}$), $\mathbf{G_{4d}}$ −63° ($OC_1{-}C_2C_3$) and 154 ($C_1C_2{-}C_3C_4$). As a result of these deviations, the carbon atoms of the dodecyloxy chains of $\mathbf{G_1}$ and $\mathbf{G_2}$ project away from the average planes defined by the arenes to which they are attached, while the carbon atoms of the dodecyloxy chains of $\mathbf{G_3}$ and $\mathbf{G_4}$ lie close to these planes.

Attempts to grow crystals of **3h** produced waxy solids.

Previously it was observed that molecules of **3a** associated in the crystal through reciprocal amide-to-amide $R_2^2(8)$ hydrogen bonding to form "one-dimensional" tapes. Lateral neighbor tapes (LNTs) of **3a** were related by screw symmetry and associated on one edge through perpendicular edge-to-center arene interactions and on the other edge through "slipped" perpendicular edge-to-center arene interactions (i.e., a methoxy hydrogen was closer to the arene centroid than the arene hydrogen) to produce "two-dimensional" sheets.[44] The data in Tables 3 and 4 and depictions of 1D-tapes and 2D-sheets from the crystal structures of compounds **3a**−**3c** (see Figure 5) attest to the fact that compounds **3b** and **3c** assemble in these two dimensions similarly to **3a** and to each other. In the case of **3b**, LNTs are related by centers of inversion and assemble on both edges through perpendicular edge-to-center arene interactions. In the case of **3c**, LNTs are related by centers of inversion and assemble on both edges through "slipped" perpendicular edge-to-center arene interactions (i.e., the butoxy hydrogens attached to C_1 were closer to the arene centroid than the arene hydrogen). While the case of **3g** is complicated by the presence of multiple conformations in the crystal, molecules of **3g** associate via reciprocal amide-to-amide $R_2^2(8)$ hydrogen bonding to form 1D-tapes, and LNTs of **3g** are related by screw symmetry and associate through perpendicular edge-to-center arene interactions (Figure 6).

Association of 2D-sheets of **3a** to form a "three dimensional" solid was previously attributed to van der Waals-driven sheet complimentarity.[44] Similar complimentarity is observed in the assembly of sheets of **3b** in which "bundled" alkoxy substituents more deeply interdigitate, maximizing van der Waals contacts. The g_+ or g_- twist about the $ArOCH_2{-}CH_2CH_2CH_3$ σ bond in molecules of **3c** precludes deep interdigitation, but such an arrangement involving fully extended alkyl chains may be possible in a crystal polymorph. To date, polymorphs of **3a**, **3b**, and **3c** have not been observed. Association of 2D-sheets of **3g** to form a 3D-solid, while more complex, clearly involves deep interdigitation of substituent alkyl chains in extended conformations in order to maximize van der Waals contacts (Figure 6).

Thermochemical Studies. Thermograms from modulated differential scanning calorimetry (DSC) of compounds **3a**−**3h** are given in the Supporting Information. Melting and freezing temperatures of compounds **3b**−**3g** are summarized in Table 5, and a plot of the observed freezing temperatures versus alkyl chain lengths appears in Figure 7. Freezing points were calculated for **3a** and **3h** using the equation of the best fit line to the data in Figure 7. Compound **3a** melted with substantial decomposition, and so its freezing temperature could not be determined. Sharp transitions were not observed for **3h** over the range 375−475 K.

■ DISCUSSION

The syntheses of **3b**−**3h** parallel the published synthesis of **3a**. Direct radical bromination of compounds **5d**−**5h** produced unacceptable mixtures of xylene methyl and ring polybromination products.[52] In these cases it was more efficient to carry out an ionic ring bromination prior to radical bromination of the methyl groups and, later in the sequence, a ring debromination. Formation of the indane rings by sequential displacements of the benzylic bromides on the way to **9b**−**9h** was inefficient. Following the first alkylation step, intermolecular alkylations were competitive with intramolecular alkylations, leading to

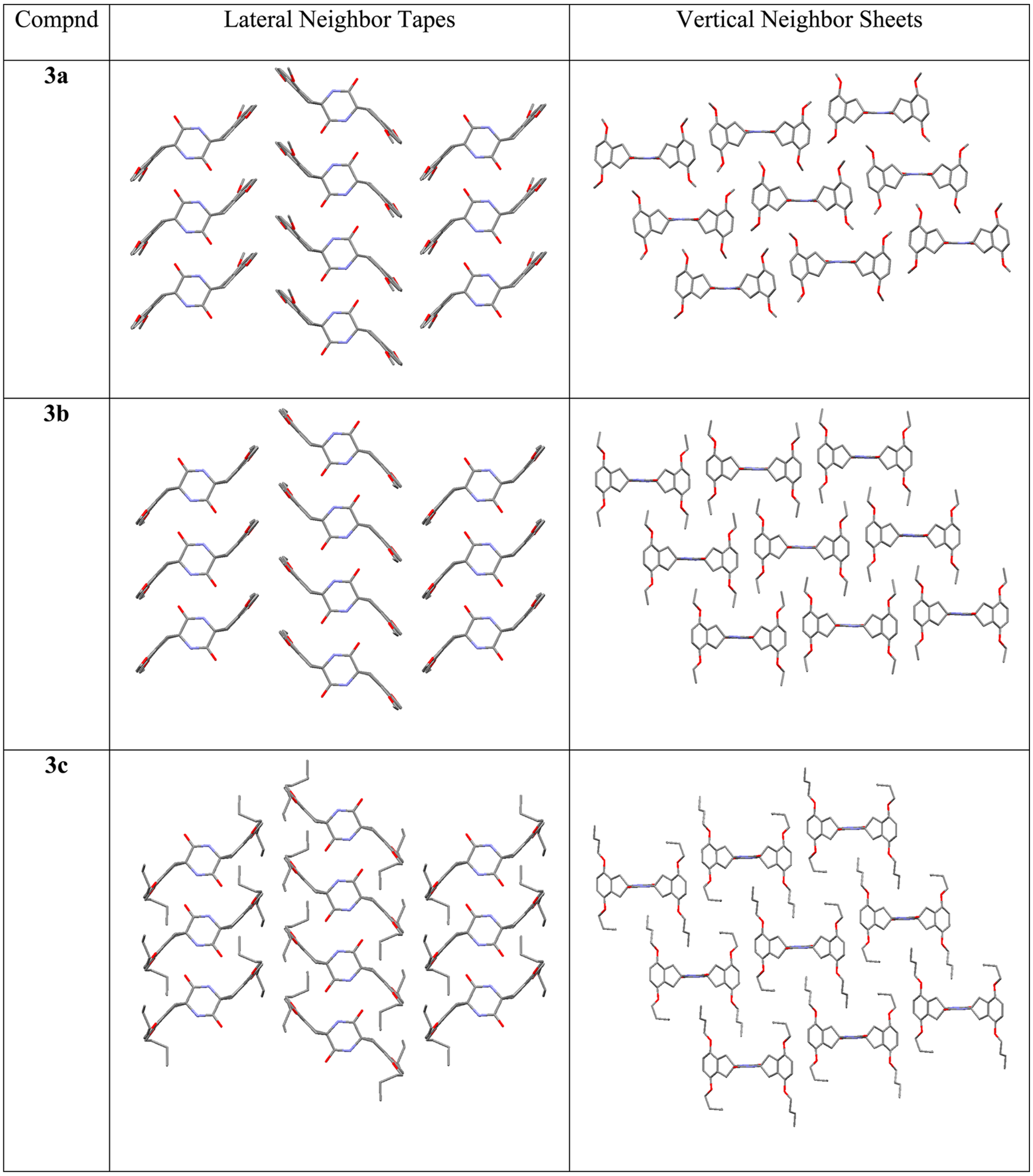

Figure 5. Tape assembly in the crystal structures of compounds **3a**−**c**. Hydrogen atoms are omitted for clarity. Left: A view of lateral neighbor tapes (LNTs) perpendicular to the hydrogen bonding axis illustrating intratape reciprocal hydrogen bonding and intertape arene interactions. Right: A view of three sheets, each consisting of three LNTs, parallel to the hydrogen bonding axis illustrating intertape arene interactions and sheet assembly via interdigitation of hydrocarbon chains.

oligomeric byproducts.[61] The remaining steps leading to dipeptides **14b**−**14h** were straightforward, and themolysis of **14b**−**14h** at 250−260 °C produced **3b**−**3h** in good to very good yields.

In prior work with **3a** and other nonpolar piperazinediones,[44] DMSO had proven to be a useful solvent for growing crystals suitable for single-crystal analysis. In the present study, solvent-free crystals of **3b** and **3c** were obtained from absolute ethanol, and solvent-free crystals of **3g** were obtained from isopropanol. Attempts to grow X-ray quality single crystals of **3d**−**3f** and **3h** from a variety of solvents were unsuccessful.

While each of the compounds **3a**−**3h** was expected to crystallize with unique structural "fine-tuning" leading to differences in the details of crystal packing, our hope was that the crystal packing of these compounds would be more similar than different, and this appears to be the case. For **3a**−**3c** and **3g**: molecules associate via reciprocal amide-to-amide $R_2^2(8)$ hydrogen bonding to form 1D-tapes; lateral neighbor tapes associate through some type of perpendicular edge-to-center arene interaction to form 2D-sheets; and sheets associate via interdigitation of bundled alkyl groups that project in "rows" away from each side of the sheet in order to maximize van der Waals contacts in the 3D-solid. An observed

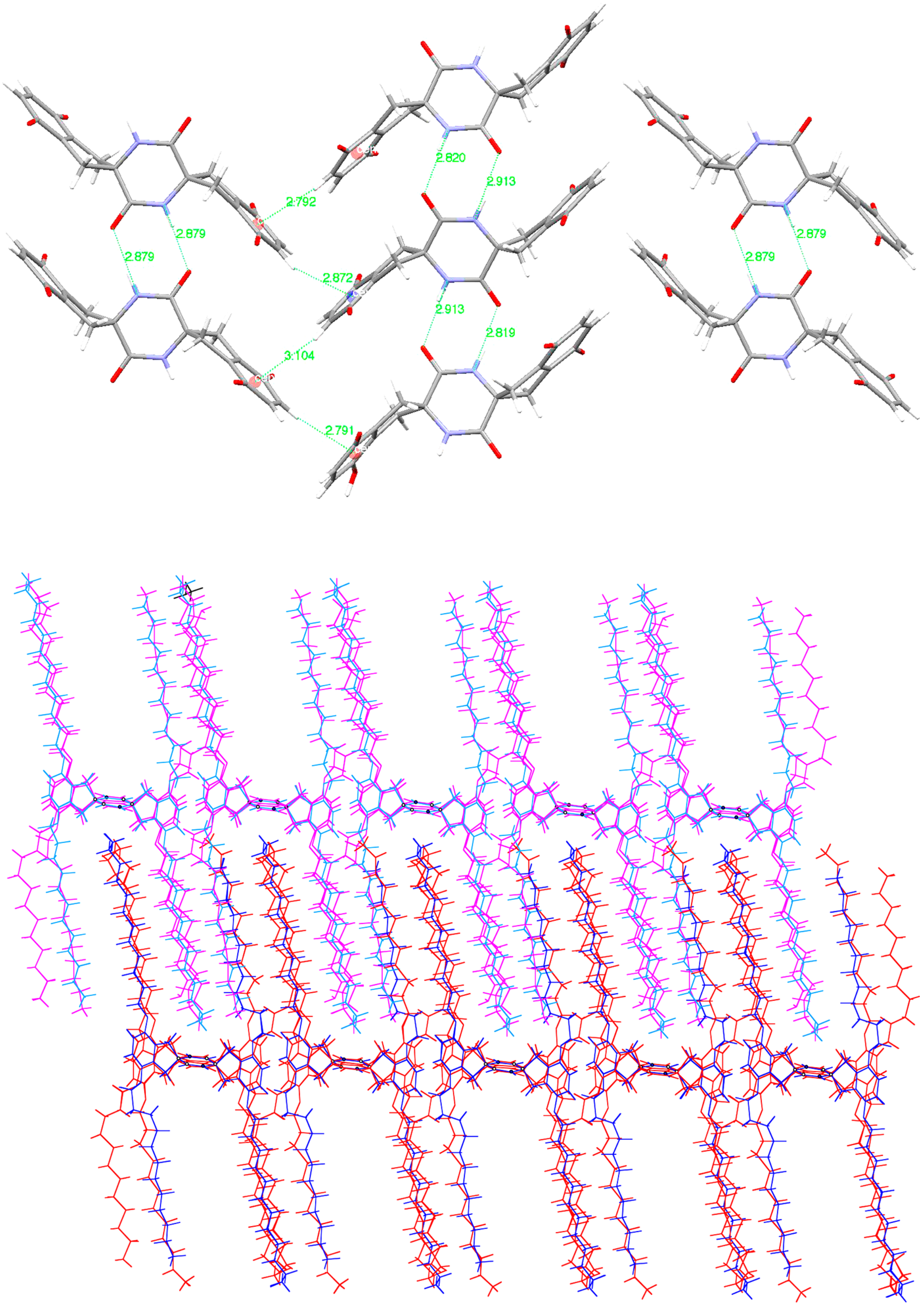

Figure 6. Tape assembly in the crystal structure of compound **3g**. Top: A view showing reciprocal amide-to-amide $R_2^2(8)$ hydrogen bonding and edge-to-center arene interactions of the molecular core. This view has been populated with conformers $\mathbf{G_1}$ (peripheral molecules) and $\mathbf{G_4}$ (central molecule). The dodecyl groups are omitted for clarity. Bottom: A view of two sheets, each consisting of five LNTs, parallel to the hydrogen bonding axis illustrating sheet assembly via interdigitation of hydrocarbon chains. The top sheet has been populated with conformers $\mathbf{G_2}$ (lavender) and $\mathbf{G_3}$ (light blue) and the bottom sheet has been populated with conformers $\mathbf{G_1}$ (red) and $\mathbf{G_4}$ (dark blue) for purposes of contrast.

crystal structure may represent a local energy minimum, not the global energy minimum for the most stable 3D assembly. Compound **3c** is of particular interest in this regard, since full extension of all four butyl chains should permit deeper interdigitation and could produce a crystal polymorph more closely resembling the packing observed for **3b**.

Table 5. Melting and Freezing Points for Piperazinediones 3a−3h[a]

compound	number of carbons in the alkoxy chains	mp (K)	fp (K)
3a	1	nd[b]	(567)[c]
3b	2	590	554
3c	4	566	544
3d	6	520	520
3e	8	511	506
3f	9	493	487
3g	12	472	464
3h	18	nd[b]	(408)[c]

[a] Measured by modulated differential scanning calorimetry; see the Supporting Information for the thermograms. [b] Not determined. [c] Calculated value, see the equation used in the legend for Figure 7.

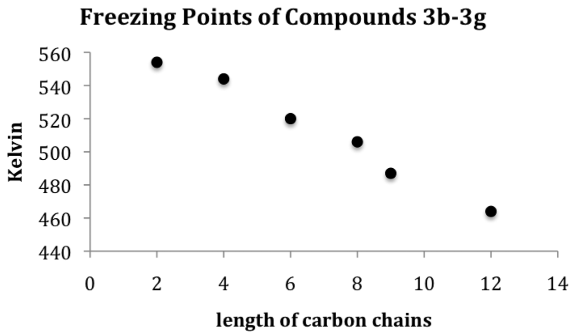

Figure 7. Graph of freezing point versus length of carbon chain for piperazinediones **3b**−**3g**. The best-fit line has the equation $y = -9.40x + 576.7$ and a correlation coefficient of 0.993.

It is interesting that the freezing temperatures for compounds **3b**−**3g** decrease as the length of the alkoxy chains increases. The crystallographic data indicate that the geometries of the hydrogen bonds, and therefore their strengths, are very similar. If hydrogen bonds of comparable strength are the last intermolecular interactions broken during melting, and thus the first intermolecular interactions formed during crystallization, the contribution of alkyl chain motion to the entropic component of the free energy could be responsible for the unexpected trend observed for the freezing temperatures. This possibility is under investigation.[62]

■ CONCLUSION

From studies of piperazinediones **3a**−**h**, we conclude (1) the thermodynamic favorability of $R_2^2(8)$ reciprocal amide hydrogen bonding results in 1D-tape formation in at least the four cases studied by X-ray crystallography, and probably in the other cases as well, given the observed linearity in the freezing temperatures of compounds **3b**−**3g** and the assumption that hydrogen bonding should be the strongest intermolecular interaction and the first interaction established passing from an isotropic to an ordered state; (2) arenes adopt perpendicular edge-to-center motifs, causing 1D-tapes to form 2D-sheets; (3) the hydrocarbon chains of the alkoxy substituents adopt more or less extended conformations perpendicular to the 2D-sheets and interdigitate to fill space between the sheets and maximize van der Waals contacts. Thus, the design model for crystal packing based on three orthogonal recognition elements appears to be valid for this set of piperazinediones. Thermally induced crystal-to-crystal or crystal-to-liquid crystal transitions may occur for some members of the set. Work is currently in progress to determine the phase behaviors of these compounds and will be reported in due course.

■ ASSOCIATED CONTENT

Ⓢ Supporting Information

General experimental section, experimental details for the synthesis and characterization of compounds leading to **3c** and **3e**−**3h**, ^{1}H and ^{13}C NMR spectra for **3b**−**3h**, differential scanning calorimetry profiles for **3a**−**3h**, and X-ray crystallographic information files (CIFs) for **3b** and **3c**. This material is available free of charge via the Internet at http://pubs.acs.org.

■ AUTHOR INFORMATION

Corresponding Author

*Address: Department of Chemistry and Biochemistry, University of Arizona, 1306 East University, Tucson, Arizona 85721-0041, USA. Phone: (520) 621-6321. Fax: (520) 621-8407. E-mail: emash@u.arizona.edu.

Notes

The authors declare no competing financial interest.

■ ACKNOWLEDGMENTS

Technical assistance from Christine Zak and Hans Zak is acknowledged. This work was supported in part by the Office of Naval Research through the Center for Advanced Multifunctional Nonlinear Optical Polymers and Molecular Assemblies, by the University of Arizona Office of the Vice President for Research, and by the Donors of the Petroleum Research Fund, administered by the American Chemical Society. The diffractometer used for data collection for compounds **3b** and **3c** was purchased with funds from NSF Grant CHE 9610374. Data collection for compound **3g** was performed at the Du Pont-Northwestern-Dow Collaborative Access Team (DND-CAT) Synchrotron Research Center located at Sector 5 of the Advanced Photon Source. DND-CAT is supported by the E.I. Du Pont de Nemours & Co., The Dow Chemical Company, the U.S. National Science Foundation through Grant DMR-9304725, and the State of Illinois through the Department of Commerce and the Board of Education Grant IBHE HECA NWU 96. Use of the Advanced Photon Source was supported by the U.S. Department of Energy, Basic Energy Sciences, Office of Science, under Contract No. W-31-109-Eng-38. We thank DND-CAT staff for their help.

■ REFERENCES

(1) *The Crystal as a Supramolecular Entity*; Desiraju, G. R., Ed.; John Wiley & Sons, Ltd: Chichester, England, 1996.

(2) *Crystal Engineering: The Design and Application of Functional Solids*; Seddon, K. R., Zaworotko, M., Eds; Kluwer Academic Publishers: Dordrecht, The Netherlands, 1999.

(3) Braga, D.; Grepioni, F. Crystal Engineering. In *Kirk-Othmer Encyclopedia of Chemical Technology*, 5th ed.; Wiley: New York, 2004; Vol. 8, pp 65−94.

(4) Wuest, J. D. *Chem. Commun.* **2005**, 5830−5837.

(5) Aakeroy, C. B; Schultheiss, N. In *Making Crystals By Design*; Braga, D., Greponi, F., Eds.; Wiley-VCH: New York, 2007; pp 209−240.

(6) Desiraju, G. R.; Vittal, J. J.; Ramanan, A. *Crystal Engineering A Textbook*; World Scientific Publishing Company: Singapore, 2011.

(7) Collings, P. J. *Liquid Crystals: Nature's Delicate Phase of Matter*, 2nd ed.; Princeton University Press: Princeton, 2002.

(8) Tschierske, C. *Chem. Soc. Rev.* **2007**, *36*, 1930−1970.

(9) Yoshizawa, A. *J. Mater. Chem.* **2008**, *18*, 2877−2889.

(10) MacDonald, J. C.; Whitesides, G. M. *Chem. Rev.* **1994**, *94*, 2383−2420.

(11) Brienne, M.-J.; Gabard, J.; Leclercq, M.; Lehn, J.-M.; Cesario, M.; Pascard, C.; Chevé, M.; Dutruc-Rosset, G. *Tetrahedron Lett.* **1994**, *35*, 8157−8160.

(12) Palacin, S.; Chin, D. N.; Simanek, E. E.; MacDonald, J. C.; Whitesides, G. M.; McBride, M. T.; Palmore, G. T. R. *J. Am. Chem. Soc.* **1997**, *119*, 11807−11816.

(13) Li, W.-R.; Kao, K.-C.; Yo, Y.-C.; Lai, C. K. *Helv. Chim. Acta* **1999**, *82*, 1400−1407.

(14) Ridvan, L.; Budesínsky, M.; Tichy, M.; Malon, P.; Závada, J.; Podlaha, J.; Císarová, I. *Tetrahedron* **1999**, *55*, 12331−12348.

(15) Luo, T-J. M.; Palmore, G. T. R. *Cryst. Growth Des.* **2002**, *2*, 337−350.

(16) Lenev, D. A.; Lyssenko, K. A.; Kostyanovsky, R. G. *Mendeleev Commun.* **2004**, *14*, 312−314.

(17) Gupta, S.; Macala, M.; Schafmeister, C. E. *J. Org. Chem.* **2006**, *71*, 8691−8695.

(18) The pentacyclic core of **1** is minimally flexible about the two cyclopentene "hinges" of the indane units and the central piperazinedione ring.

(19) In June 2012, 144 nitrogen-unsubstituted non-ionic piperazinediones with 3D coordinates were retrieved from the Cambridge Structural Database (CSD, version 5.33, see Allen, F. H. *Acta Crystallogr. Sect. B* **2002**, *58*, 380−388); 64% possess one-dimensional "ladder-like" tapes (i), 4% form non-reciprocal hydrogen bonded networks (ii), and 32% develop alternate hydrogen bonded structures involving piperazinedione side chains and/or included molecules.

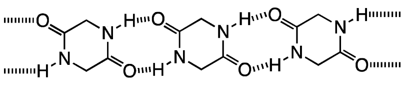

i

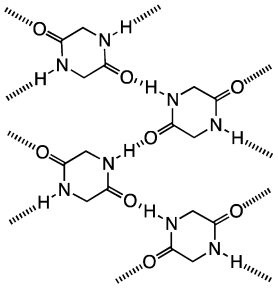

ii

(20) Kitaigorodsky, A. I. *Molecular Crystals and Molecules*; Academic Press: New York, 1973.

(21) Depero, L. E. *Adv. Mol. Struct. Res.* **1995**, *1*, 303−337.

(22) Perlstein, J. *NATO Sci. Ser. C* **1999**, *538*, 23−42.

(23) Desiraju, G. R. *Nat. Mater.* **2002**, *1*, 77−79.

(24) Organic zeolites are exceptions; see Hertzsch, T.; Hulliger, J.; Weber, E.; Sozzani, P. In *Encyclopedia of Supramolecular Chemistry*; Taylor and Francis: New York, 2007; pp 996−1005, and references cited therein.

(25) Hunter, C. A.; Lawson, K. R.; Perkins, J.; Urch, C. J. *J. Chem. Soc., Perkin Trans. 2* **2001**, 651−669.

(26) Waters, M. L. *Curr. Opin. Chem. Biol.* **2002**, *6*, 736−741.

(27) The terms "parallel center-to-center", "parallel edge-to-center", and "perpendicular edge-to-center" will be used to describe arene interaction types herein. Other terms that have been used to designate arene interaction motifs include, for parallel center-to-center (iii), face-to-face, face-to-face stacked, parallel stacked, and stacked; for parallel edge-to-center (iv) face-to-face center-to-edge, parallel offset, offset stacked, and offset nonstacked; and for perpendicular edge-to-center (v) edge-to-face, edge-face, herringbone, and T-type.

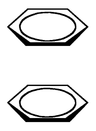

iii

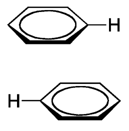

iv

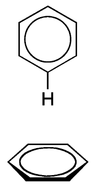

v

(28) Reichenbächer, K.; Süss, H. I.; Hulliger, J. *Chem. Soc. Rev.* **2005**, *34*, 22−30.

(29) Dai, C.; Nguyen, P.; Marder, T. B.; Scott, A. J.; Clegg, W.; Viney, C. *J. Chem. Soc., Chem. Commun.* **1999**, 2493−2494.

(30) Gung, B. W.; Xue, X.; Zou, Y. *J. Org. Chem.* **2007**, *72*, 2469−2475.

(31) Carroll, W. R.; Pellechia, P.; Shimizu, K. D. *Org. Lett.* **2008**, *10*, 3547−3550.

(32) Cozzi, F.; Annunziata, R.; Benaglia, M.; Cinquini, M.; Raimondi, L.; Baldridge, K. K.; Siegel, J. S. *Org. Biomol. Chem.* **2003**, *1*, 157−162.

(33) Budzianowski, A.; Katrusiak, A. *Acta Crystallogr., Sect. B* **2006**, *62*, 94−101 and prior structures.

(34) Oddershede, J.; Larsen, S. *J. Phys. Chem. A* **2004**, *108*, 1057−1063 and prior structures.

(35) Marciniak, B.; Pavlyuk, V. *Mol. Cryst. Liq. Cryst. Sci. Technol., Sect. A* **2002**, *373*, 237−250 and prior structures.

(36) Umezawa, Y.; Tsuboyama, S.; Honda, K.; Uzawa, J.; Nishio, M. *Bull. Chem. Soc. Jpn.* **1998**, *71*, 1207−1213.

(37) Kim, E.; Paliwal, S.; Wilcox, C. S. *J. Am. Chem. Soc.* **1998**, *120*, 11192−11193.

(38) Nakamura, K.; Houk, K. N. *Org. Lett.* **1999**, *1*, 2049−2051.

(39) Ribas, J.; Cubero, E.; Luque, F. J.; Orozco, M. *J. Org. Chem.* **2002**, *67*, 7057−7065.

(40) Carver, F. J.; Hunter, C. A.; Livingstone, D. J.; McCabe, J. F.; Seward, E. M. *Chem. Eur. J.* **2002**, *8*, 2847−2859.

(41) Cockroft, S. L.; Hunter, C. A. *Chem. Commun.* **2006**, 3806−3808.

(42) Fischer, F. R.; Schweizer, W. B.; Diederich, F. *Chem. Commun.* **2008**, 4031−4033.

(43) Tewari, A. K.; Dubey, R. *Bioorg. Med. Chem.* **2008**, *16*, 126−143.

(44) Williams, L. J.; Jagadish, B.; Kloster, R. A.; Lyon, S. R.; Carducci, M. D.; Mash, E. A. *Tetrahedron* **1999**, *55*, 14281−14300.

(45) Williams, L. J.; Jagadish, B.; Lansdown, M. G.; Carducci, M. D.; Mash, E. A. *Tetrahedron* **1999**, *55*, 14301−14322.

(46) Kaneko, F.; Sakashita, H.; Kobayashi, M.; Kitagawa, Y.; Matsuura, Y.; Suzuki, M. *Acta Crystallogr., Sect. C* **1994**, *50*, 245−247.

(47) Bryan, R. F.; Hartley, P.; Miller, R. W.; Shen, M.-S. *Mol. Cryst. Liq. Cryst.* **1980**, *62*, 281−310.

(48) For a preliminary communication, see Kloster, R. A.; Carducci, M. D.; Mash, E. A. *Org. Lett.* **2003**, *5*, 3683−3686.

(49) The General Experimental Section is located in the Supporting Information that accompanies this paper.

(50) Röhrich, J.; Müllen, K. *J. Org. Chem.* **1992**, *57*, 2374−2379.

(51) Purchased from Aldrich Chemical Co.

(52) Gruter, G-J. M.; Akkerman, O. S.; Bickelhaupt, F. *J. Org. Chem.* **1994**, *59*, 4473−4481.

(53) Kotha, S.; Kuki, A. *Tetrahedron Lett.* **1992**, *33*, 1565−1568.

(54) Kotha, S.; Brahmachary, E. *J. Org. Chem.* **2000**, *65*, 1359−1365.

(55) Castro, B.; Dormoy, J.-R.; Dourtoglou, B.; Evin, G.; Selve, C.; Ziegler, J.-C. *Synthesis* **1976**, 751−752.

(56) IUPAC-IUB Commission on Biochemical Nomenclature, *Biochemistry* **1970**, *9*, 3471−3479.

(57) Karlström, G.; Linse, P.; Wallqvist, A.; Jönsson, B. *J. Am. Chem. Soc.* **1983**, *105*, 3777−3782.

(58) Burley, S. K.; Petsko, G. A. *J. Am. Chem. Soc.* **1986**, *108*, 7995−8001.

(59) Jorgensen, W. L.; Severance, D. L. *J. Am. Chem. Soc.* **1990**, *112*, 4768−4774.

(60) Hobza, P.; Selzle, H. L.; Schlag, E. W. *J. Am. Chem. Soc.* **1994**, *116*, 3500−3506.

(61) Ridvan, L.; Zavada, J. *Tetrahedron* **1997**, *53*, 14793−14806.

(62) Weatherhead-Kloster, R. A.; Selby, H. D.; Miller, W. B., III; Mash, E. A. *J. Org. Chem.* **2005**, *70*, 8693−8702.